Outer trench-slope faulting and the 2011 M_w 9.0 off the Pacific coast of Tohoku Earthquake

Thorne Lay[1], Charles J. Ammon[2], Hiroo Kanamori[3], Marina J. Kim[1], and Lian Xue[1]

[1]*University of California Santa Cruz, Santa Cruz, California 95064, USA*
[2]*The Pennsylvania State University, University Park, Pennsylvania 16802, USA*
[3]*California Institute of Technology, Pasadena, California 91125, USA*

(Received April 7, 2011; Revised May 6, 2011; Accepted May 7, 2011; Online published September 27, 2011)

The 11 March 2011 off the Pacific coast of Tohoku Earthquake (M_w 9.0) produced megathrust displacements of at least 40 m. The resulting tsunami devastated the Honshu coast southwest of regions struck by earthquake-generated tsunami in 1611, 1896 and 1933. The 1896 Meiji-Sanriku earthquake was also an underthrusting earthquake, but the 1933 Sanriku-oki earthquake was a trench-slope normal faulting event; both generated inundation heights of 10 to 25 m along the coast of Iwate prefecture. Possible occurrence of a great outer trench-slope earthquake seaward of the 2011 Tohoku Earthquake along a southwestward extension of the 1933 fault zone is a concern. The second largest 2011 aftershock, an outer rise M_w 7.7 normal faulting earthquake occurred near the southern end of the 1933 rupture. Additional aftershock activity has been distributed along a trend below the trench and diffusely spread in the outer rise, seaward of the megathrust region where the largest slip occurred. Coulomb stress perturbations of at least 5–10 bars are calculated for outer rise normal fault geometries for mainshock slip models. Whether a future great trench slope event will occur is uncertain, but the potential tsunamigenic hazard can be gauged by the huge inundations accompanying the 1933 rupture.
Key words: Great normal faults, tsunami, 1933 Sanriku-oki, outer rise earthquakes.

1. Introduction

When a large interplate thrusting earthquake occurs on a subduction zone megathrust, it is common for shallow intraplate extensional-faulting aftershock activity to be detected within the subducting plate beneath the seaward trench slope or outer rise (e.g., Stauder, 1968; Christensen and Ruff, 1988). This outer trench-slope aftershock activity has been particularly notable up-dip of great earthquakes such as the 1960 Chile (M_w 9.5), 1965 Aleutians (M_w 8.6), 1963 Kuril (M_w 8.3), 2004 Sumatra (M_w 9.2) and 2010 Chile (M_w 8.8) events. Typically, the largest magnitude trench-slope aftershocks are much smaller than the underthrusting mainshocks, and the primary interest in these events has been for quantifying aspects of the stress variations associated with the seismic cycle of megathrust faults and the relative importance of dynamic and bending stresses (e.g., Dmowska *et al.*, 1988; Lay *et al.*, 1989; Taylor *et al.*, 1996). However, some great extensional faulting events have happened in the outer trench slope environment with no proximate large thrust event, such as the 1977 Sumba (M_w 8.4) (Lynnes and Lay, 1988) and 2009 Samoa (M_w 8.1) (Lay *et al.*, 2010) earthquakes which occurred seaward of what appear to be seismically weakly-coupled subduction zones. For these latter events, slab-pull/bending stresses appear to play important roles, with no obvious influence from interplate seismic stress cycles, although as yet undetected slow earthquakes on the megathrust may occur in these environments.

Of particular relevance here are two great events that have struck the outer rise subsequent to great interplate ruptures located in the shallow portion of their megathrust faults. The 1933 Sanriku-oki (M_w 8.6) event (Kanamori, 1971) ruptured seaward of the 1896 Meiji-Sanriku tsunami earthquake ($M \sim 8.5$) (Kanamori, 1972; Tanioka and Satake, 1996), and the 13 January 2007 Kuril (M_w 8.1) earthquake ruptured seaward of the 16 November 2006 Kuril (M_w 8.4) underthrusting earthquake (Ammon *et al.*, 2008). Both of these sequences involve regions of somewhat unusual interplate coupling.

The megathrust region that ruptured in the 1896 Sanriku earthquake was near the trench (Fig. 1) and weak short-period seismic waves were radiated during the faulting, possibly because the event had a low rupture velocity. The region of the megathrust down-dip of the 1896 rupture appears to be very weakly coupled, with sparse back-ground seismicity and a lack of large historic near-coast earthquakes (e.g., Kanamori *et al.*, 2006; Gamage *et al.*, 2009). The 1933 intraplate rupture did radiate large amplitude short-period seismic waves, as is typical for trench slope and outer rise faulting (Lay *et al.*, 2010). The depth extent of the rupture is not well resolved, but appears to extend from the surface to depths of at least 25 km, and perhaps significantly deeper into the lithospheric mantle (Kanamori, 1971). Aftershock activity is still observed in the region and suggests a steeply dipping plane plunging toward the trench

doi:10.5047/eps.2011.05.006

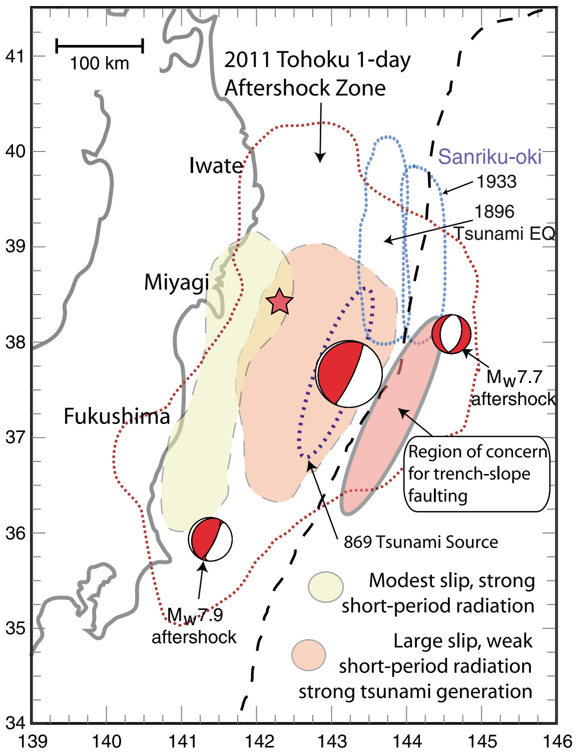

Fig. 1. Map of the 2011 Tohoku rupture attributes and historic large earthquakes along the up-dip region of the Japan subduction zone. The long dashed curve indicates the position of the trench. The red star is the USGS epicentral location. Frequency-dependent attributes of the 2011 mainshock rupture inferred from short-period and broadband seismic and geodetic analyses are indicated (Koper *et al*., 2011). The 1 day aftershock zone for the 2011 event is delimited by the red dotted curve with the global centroid moment tensor focal mechanisms for the mainshock, the 11 March 2011 M_w 7.9 thrust aftershock and the large 11 March 2011 M_w 7.7 outer rise aftershock being shown. The pink ellipse indicates the trench slope environment for which there is concern about future tsunamigenic normal faulting.

(Gamage *et al*., 2009). The 1896 and 1933 earthquakes both generated substantial and deadly tsunamis, of up to 25 m along the coast of Iwate prefecture (Hatori, 1969).

The 2006 Kuril event ruptured the up-dip margin of the megathrust further seaward than typical great earthquakes along the Kuril island arc, in a distinctive region where the trench narrows, the volcanic arc is disrupted, and a fore-arc basin is present (Lay *et al*., 2009). The thrust event ruptured about 200 km along strike of the arc and immediately activated normal faulting activity in the trench slope which decayed slowly over time until the great 2007 Kuril intraplate event occurred, radiating with strong short-period seismic wave energy. While the moment of the 2007 event was about 50% that of the 2006 event and the far-field tsunami was correspondingly smaller, the 2007 event produced stronger shaking in Japan due to having higher moment-scaled energy release (Ammon *et al*., 2008). While the 37-year time separation between the Sanriku events in 1896 and 1933 is substantial, the Kuril doublet was separated by only about 60 days. A much smaller pair of thrust (M_w 7.2, 16 August 2005) and outer rise normal (M_w 7.0, 14 November 2005) events ruptured in the region of interest here, separated by 90 days (Hino *et al*., 2009). The processes that control the relative timing of these events are not known specifically, but candidates include viscous relaxation of the lower part of the slab, poroelastic response in the trench slope region to the change in stresses from the initial thrust event, and visco-elastic deformation of the subducting plate (Lay *et al*., 2009).

The 11 March 2011 Tohoku Earthquake (M_w 9.0) ruptured the Japan subduction zone directly south of the 1896 and 1933 Sanriku-oki earthquakes (Fig. 1). We consider the nature of the faulting in this great event and address the concern about potential for great extensional faulting in the outer trench slope or outer rise region seaward of the rupture zone (Fig. 1), and associated potential for another large tsunamigenic event in this region.

2. The 11 March 2011 Rupture

The rupture process of the 2011 Tohoku Earthquake is under active investigation, but numerous studies have quantified basic attributes of the source process. We draw upon two finite-fault models for the coseismic faulting during the mainshock (Fig. 2). The first, denoted P-Mod, is derived from least-squares inversion of teleseismic P waves using a layered source region velocity structure adapted from Takahashi *et al.* (2004). Details about the corresponding inversion process are presented in Lay *et al.* (2011c). The second, denoted J-Mod, is a joint inversion of teleseismic P waves, short-arc Rayleigh wave (R_1) relative source time functions, and regional continuous GPS recordings (Ammon *et al*., 2011). A half-space was used in J-Mod for constructing the slip solution from the seismic moment distribution. The reduced rigidity at shallow depth in the P-Mod structure enhances up-dip slip relative to J-Mod. The fault models differ in their resolution of roughness of the slip distribution but both concentrate seismic moment (and slip) up-dip of the hypocenter; have comparable seismic moments of 3.6×10^{22} N m (J-Mod) to 4.1×10^{22} N m (P-mod), compatible with long-period determinations of seismic moment ($\sim3.9\times10^{22}$ N m; Ammon *et al*., 2011); and have maximum slips of about 40 m, with average slip of about 15 m over the regions of the fault models where slip is well-resolved. Even larger slips at very shallow depth are proposed by other inversions (e.g., Lay *et al*., 2011c), and the calculations based on these models can be viewed as a conservative estimate for stress changes. The rupture velocity is low, 1.5 km/s, in the region of the main slip, which may indicate the presence of sediments or fluids in the fault zone. This low rupture velocity is characteristic of tsunami earthquakes (Kanamori and Kikuchi, 1993; Tanioka and Seno, 2001; Polet and Kanamori, 2000; Bilek and Lay, 2002; Ammon *et al*., 2006), and may correspond to why the 1896 event to the north also ruptured slowly.

Whether large coseismic slip extended all the way to the trench or not is still under investigation. The area of strong slip overlaps the estimated source region of the 869 Jogan tsunami (Minoura *et al*., 2001), but whether the ∼50–100 km wide shallowest portion of the megathrust remains unbroken, at least in some regions, is still to be resolved. This is important relative to the possibility of slow megathrust tsunami earthquakes in the shallow region up-dip of a large interplate rupture, as has occurred in the Kuril islands (Pelayo and Wiens, 1992) and along Sumatra (Kanamori

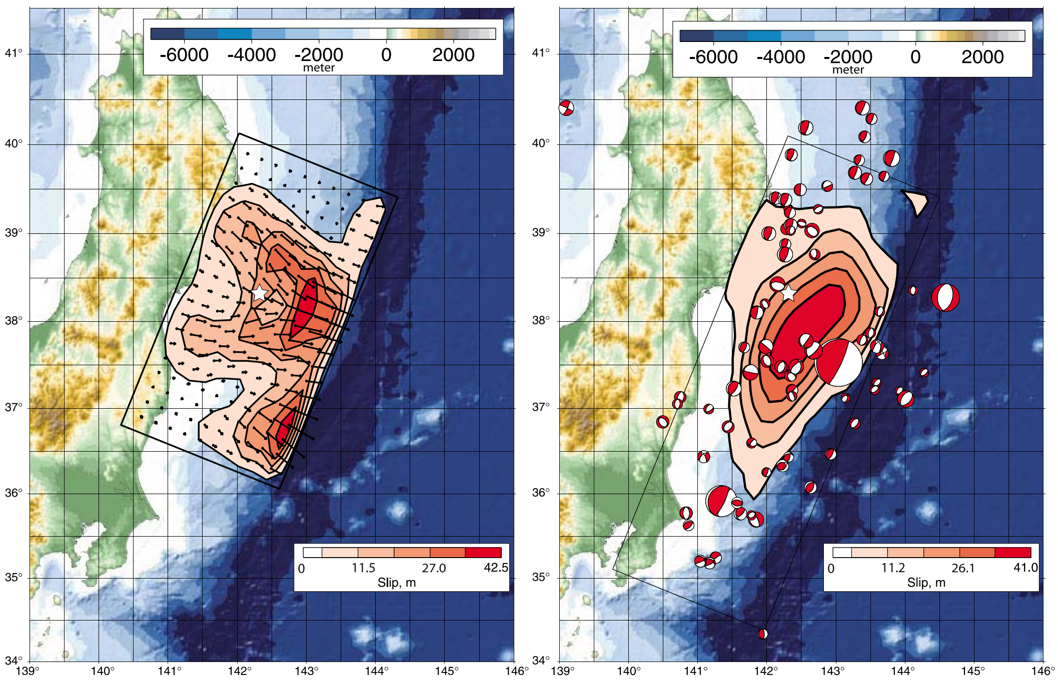

Fig. 2. Maps of slip distributions for two finite-faulting models derived from teleseimic P-waves (left) and joint inversion of P waves, Rayleigh waves and continuous GPS observations (right, adapted from Ammon *et al.*, 2011). The P wave inversion model has variable rake of the subfaults, indicated by the small vectors; the joint inversion has uniform rake of 85°. The global centroid moment tensor (GCMT) solutions for the mainshock and aftershocks are shown on the right map.

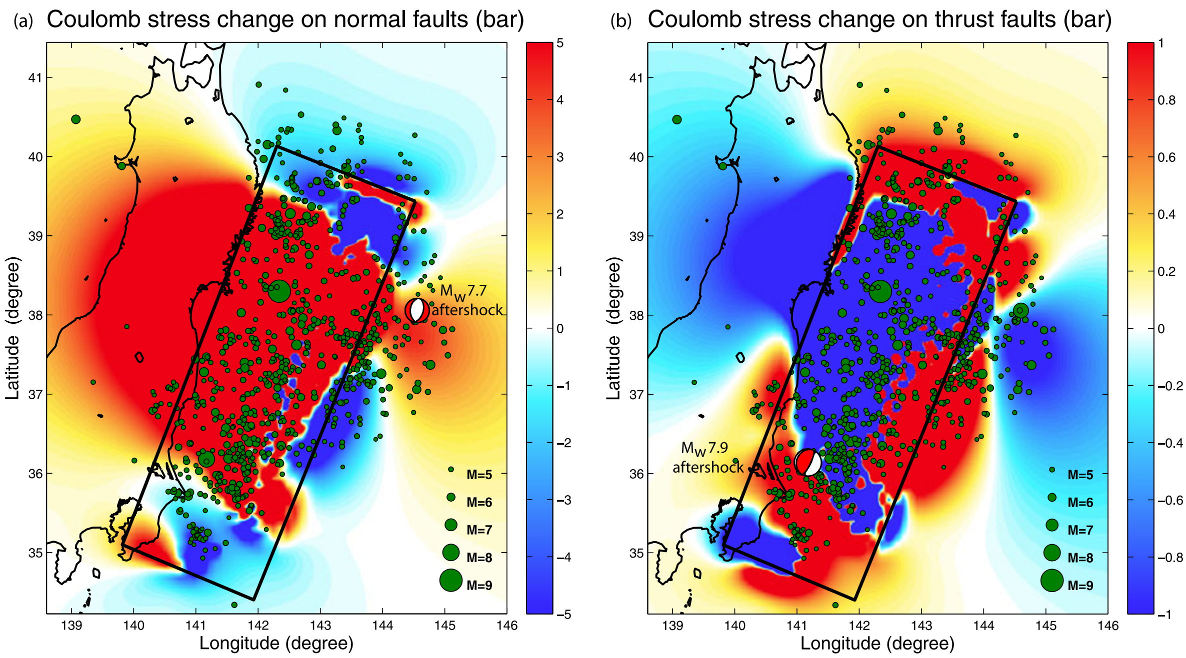

Fig. 3. Maps of the Coulomb stress change predicted for the joint P wave, Rayleigh wave and continuous GPS inversion in Fig. 2. The margins of the latter fault model are indicated by the box. Two weeks of aftershock locations from the U.S. Geological Survey are superimposed, with symbol sizes scaled relative to seismic magnitude. (a) The Coulomb stress change averaged over depths of 10–15 km for normal faults with the same westward dipping fault plane geometry as the M_w 7.7 outer rise aftershock, for which the global centroid moment tensor mechanism is shown. (b) Similar stress changes for thrust faults with the same geometry as the mainshock, along with the M_w 7.9 thrusting aftershock to the south, for which the global centroid moment tensor is shown.

et al., 2010; Lay *et al.*, 2011a). Comparisons of observations of deep-water tsunami recordings with predictions of the fault models support up-dip concentration of slip for the mainshock, perhaps with large slip all the way to the trench (Lay *et al.*, 2011b, c). The seismic radiation from the megathrust does indicate relatively strong short-period radiation from deeper than the hypocenter, but with smaller displacements, as indicated in Fig. 1 (Koper *et al.*, 2011).

We consider the models in Fig. 2 to be representative of the basic features of the mainshock rupture while conveying the current uncertainties in precise placement and magnitude of the slip. We use these models to evaluate first-order changes in the outer trench-slope and outer-rise environments following the great thrust event.

3. Stress Change and Aftershocks in the Outer Rise and Trench Slope

Evaluating the potential hazard of trench slope and outer rise faulting is very difficult, as we do not know ambient stress conditions or even precise distribution of faults in the intraplate region up-dip of the megathrust faulting. We consider changes in stress on two fault orientations to give some guidance as to likely perturbations associated with the underthrusting events. We estimate the stress perturbations using Coulomb 3, software produced by S. Toda, R. Stein, J. Lin and V. Sevilgen. Our implementation assumes a half-space with a finite fault with subfault geometries and slip given by either of the two models shown in Fig. 2. We calculate average stress changes over depths of 10–15 km for two fault geometries; a normal faulting geometry given by the westward dipping plane of the large M_w 7.7 aftershock (Fig. 1) located in the outer rise (strike 182° dip 42° rake −100°; Global Centroid Moment Tensor (GCMT)) and a thrust fault geometry the same as the mainshock (strike 202° dip 12° rake 90°; GCMT). Similar stress change magnitudes and spatial patterns were found for the eastward dipping plane of the normal fault, so they are not shown here. A conventional friction coefficient of 0.4 is assumed for the cases shown here. Very similar results with stress change differences of only ±1 bar were found using higher friction coefficients of 0.8–0.85.

The resulting calculations are shown for the J-Mod solution in Fig. 3, with very similar basic features being found for the P-Mod. The patterns of Coulomb stress change on the two fault geometries are shown relative to the mainshock rupture model and the distribution of 2-week aftershock locations from the U.S. Geological Survey is superimposed. The regions where stress changes favor increased driving stress for faulting on the two geometries are indicated in red. The normal fault geometry indicates increases in Coulomb stress of about 5 bars near the location of the large outer rise aftershock east of the hypocenter, and a large region of extension of the upper plate resulting from the thrusting. The Coulomb stress changes persist with depth, and are about 10 bars at 50 km depth and 5 bars at 100 km depth beneath the outer trench slope. The aftershock activity just seaward of the fault model lies under the trench, and it is unclear whether the faulting is shallow thrusting near the toe of the upper wedge or intraplate extensional activity, but available GCMT solutions do show mostly extensional faulting there as well as above the fault plane (Fig. 2). Stress perturbations grow to tens and even hundreds of bars for the normal faulting geometry close to the edge of the fault, but this is not reliable given the uncertainties in the slip models.

For the thrust faulting geometry, increases in Coulomb stress of up to several bars are found along strike of the main slip zones, and the largest aftershock, an M_w 7.9 event (06:15:40.88 UTC, 36.18°N 141.17°E; USGS) is located near the southwestern end of the coseismic slip zone in a region of increased Coulomb stress. There is obvious concern about future thrust faulting at shallower depth along the 200-km long segment extending southwest to the Sagami Trough where there was a modest increase in driving Coulomb stress. The other region of increased driving stress for thrusting is along the up-dip edge of the fault model away from the primary thrust zone. This could plausibly involve shallow thrusting events in the toe, but again, the mechanisms for many of these events are not known and the larger ones tend to be extensional.

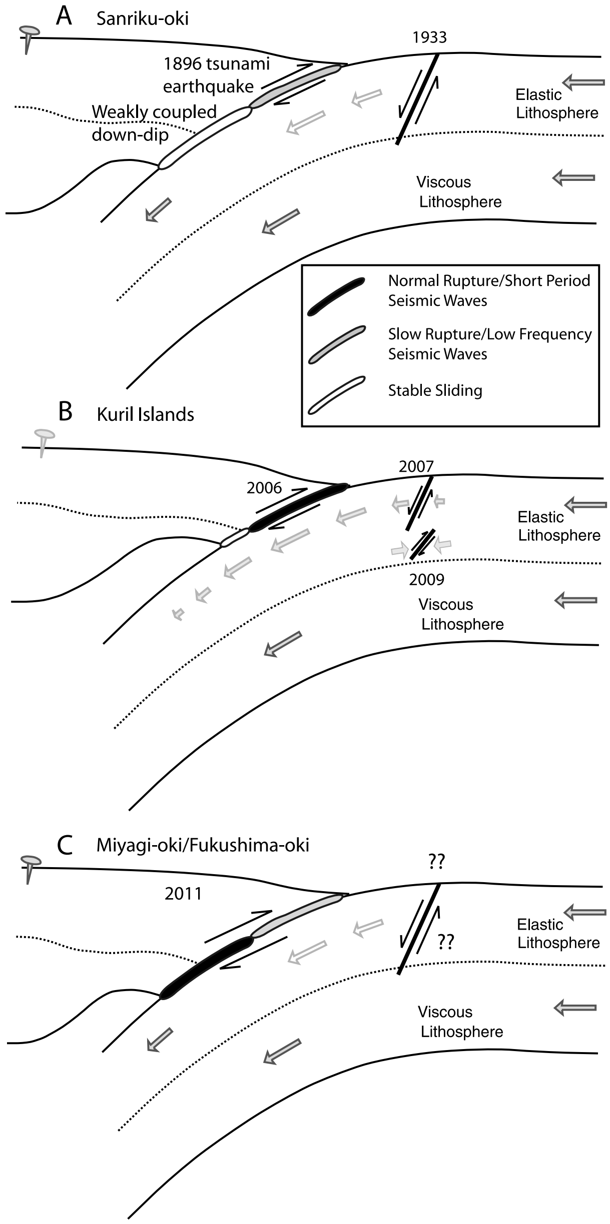

Fig. 4. Schematic cross-sections of the A) Sanriku-oki, B) Kuril and C) Miyagi-oki subduction zones where great interplate thrust events have been followed by great trench slope or outer rise extensional events (in the first two cases) and concern about that happening in the case of the 2011 event.

The P-mod predictions of Coulomb stress are similar in spatial pattern, but somewhat higher stress changes by up to a factor of two are predicted near the trench due to larger slip in the model at shallow depth. Lower stress changes in the outer rise are predicted for models with slip at greater depth along the megathrust.

4. Discussion

It is not surprising that Coulomb stress changes indicate increased driving force on outer rise normal fault geometries, as there has indeed been activation of offshore faults already in the aftershock sequence, including the second largest aftershock to date. This is commonly observed, and has, though rarely, lead to great trench slope faulting (Fig. 4). In this case, the large slip on the megathrust at relatively shallow depths does predict stresses changes on the order of 5–10 bar, which is larger than typical values of $\sim$1 bar associated with most large earthquakes. Whether or not this is significant in terms of potential great earthquake faulting in the outer trench depends on many unknowns; what are the precise outer trench slope fault geometries along this stretch of the subduction zone; are there any through-going structures that could support a rupture the size of the 1933 Sanriku-oki event; are any such faults near their failure thresholds such that the stress perturbations have significantly advanced them toward failure?

It is difficult to address these unknowns, but there is certainly some basis for concern about the possibility of a large 1933-like event near the trench. The similarities of the failure process of the up-dip region of the megathrust to the 1896 tsunami earthquake, the similiarity of physiographic structure with the arc to the north, the large mainshock slip and stress changes produced by the event, and the recognition of a few examples of past pairing of great thrusts and extensional events all contribute to the concern.

However, the lack of great extensional events following numerous other great megathrust failures in other environments urges caution in considering this concern. With no documentation of great outer rise tsunamigenic events in this area since the time of the 869 megathrust rupture (Iida *et al.*, 1967), it is possible either that the region cannot support great normal faulting or that it has large strain accumulations that would enable such faulting. At any rate, it is prudent that evaluation of tsunami hazard for the future along the Miyagi-oki and Fukushima-oki margins should take into consideration the history of great outer rise normal faulting just to the north and the possible accentuating effects of the great 2011 Tohoku Earthquake.

Acknowledgments. This work made use of GMT, SAC and Coulomb 3 software. The IRIS DMS data center was used to access the seismic data. Continuous GPS data processed with 30 s sampling were provided by the ARIA team at JPL and Caltech. This work was supported by NSF grants EAR0635570, EAR0948660, and USGS Award Number 05HQGR0174. We thank T. Seno and an anonymous reviewer for constructive reviews.

References

Ammon, C. J., H. Kanamori, T. Lay, and A. A. Velasco, The 17 July 2006 Java tsunami earthquake, *Geophys. Res. Lett.*, **233**, L234308, doi:10.10239/2006GL028005, 2006.

Ammon, C. J., H. Kanamori, and T. Lay, A great earthquake doublet and seismic stress transfer cycle in the central Kuril islands, *Nature*, **451**, 561–566, 2008.

Ammon, C. J., T. Lay, H. Kanamori, and M. Cleveland, A rupture model of the 2011 off the Pacific coast of Tohoku Earthquake, *Earth Planets Space*, **63**, this issue, 693–696, 2011.

Bilek, S. L. and T. Lay, Tsunami earthquakes possibly widespread manifestations of frictional conditional stability, *Geophys. Res. Lett.*, **29**(14), doi:10.1029/2002GL015215, 2002.

Christensen, D. H. and L. J. Ruff, Seismic coupling and outer-rise earthquakes, *J. Geophys. Res.*, **93**, 13,421–13,444, 1988.

Dmowska, R., J. R. Rice, L. C. Lovison, and D. Josell, Stress transfer and seismic phenomena in coupled subduction zones during the earthquake cycle, *J. Geophys. Res.*, **93**, 7869–7884, 1988.

Gamage, S. S. N., N. Umino, A. Hasegawa, and S. H. Kirby, Offshore double-planed shallow seismicity in the NE Japan forearc region revealed by sP depth phases recorded by regional networks, *Geophys. J. Int.*, doi:10.1111/j.1365–246x.2009.04048.x, 2009.

Hatori, T., Dimensions and geographic distribution of tsunami sources near Japan, *Bull. Earthq. Res. Inst.*, **47**, 185–214, 1969.

Hino, R., R. Azuma, Y. Ito, Y. Yamamoto, K. Suzuki, H. Tsushima, S. Suzuki, M. Miyashita, T. Tomori, M. Arizono, and G. Tange, Insight into complex rupturing of the immature bending normal fault in the outer slope of the Japan Trench from aftershocks of the 2005 Sanriku earthquake (M_w = 7.0) located by ocean bottom seismometry, *Geochem. Geophys. Geosyst.*, **10**, Q07O18, doi:10.1029/2009GC0 02415, 2009.

Iida, K., D. C. Cox, and G. Pararas-Carayannis, Preliminary catalog of tsunamis occurring in the Pacific Ocean, *Data Report 5*, HIG-6 7–10, Hawaii Inst. Geophys. Univ. Hawaii, Honolulu, pp. 261, 1967.

Kanamori, H., Seismological evidence for a lithospheric normal faulting; the Sanriku earthquake of 1933, *Phys. Earth Planet. Inter.*, **4**, 289–300, 1971.

Kanamori, H., Mechanism of tsunami earthquakes, *Phys. Earth Planet. Inter.*, **6**, 346–359, 1972.

Kanamori, H. and M. Kikuchi, The 1992 Nicaragua earthquake: A slow tsunami earthquake associated with subducted sediments, *Nature*, **361**, 714–716, 1993.

Kanamori, H., M. Miyazawa, and J. Mori, Investigation of the earthquake sequence off Miyagi prefecture with historical seismograms, *Earth Planets Space*, **58**, 1533–1541, 2006.

Kanamori, H., L. Rivera, and W. H. K. Lee, Historical seismograms for unraveling a mysterious earthquake: The 1907 Sumatra earthquake, *Geophys. J. Int.*, **183**, 358–374, doi:10.1111/j.1365-246X.2010.04731.x, 2010.

Koper, K. D., A. R. Hutko, T. Lay, C. J. Ammon, and H. Kanamori, Frequency-dependent rupture process of the 2011 M_w 9.0 Tohoku Earthquake: Comparison of short-period *P* wave backprojection images and broadband seismic rupture models, *Earth Planets Space*, **63**, this issue, 599–602, 2011.

Lay, T., L. Astiz, H. Kanamori, and D. H. Christensen, Temporal variation of large intraplate earthquakes in coupled subduction zones, *Phys. Earth Planet. Inter.*, **54**, 258–312, 1989.

Lay, T., H. Kanamori, C. J. Ammon, A. R. Hutko, K. Furlong, and L. Rivera, The 2006-2007 Kuril Islands great earthquake sequence, *J. Geophys. Res.*, **114**, B113208, doi:10.1029/2008JB006280, 2009.

Lay, T., C. J. Ammon, H. Kanamori, L. Rivera, K. Koper, and A. R. Hutko, The 29 September 2009 Great Samoa earthquake, *Nature*, **466**, 964–968, doi:10.1038/nature09214, 2010.

Lay, T., C. J. Ammon, H. Kanamori, Y. Yamazaki, K. F. Cheung, and A. R. Hutko, The 25 October 2010 Mentawai tsunami earthquake (M_w 7.8) and the tsunami hazard presented by shallow megathrust ruptures, *Geophys. Res. Lett.*, **38**, L06302, doi:10.1029/2010G, 2011a.

Lay, T., Y. Yamazaki, C. J. Ammon, K. F. Cheung, and H. Kanamori, The 2011 M_w 9.0 off the Pacific coast of Tohoku Earthquake: Comparison of deep-water tsunami signals with finite-fault rupture model predictions, *Earth Planets Space*, **63**, this issue, 797–801, 2011b.

Lay, T., C. J. Ammon, H. Kanamori, L. Xue, and M. J. Kim, Possible large near-trench slip during the 2011 M_w 9.0 off the Pacific coast of Tohoku Earthquake, *Earth Planets Space*, **63**, this issue, 687–692, 2011c.

Lynnes, C. S. and T. Lay, Source process of the great 1977 Sumba earthquake, *J. Geophys. Res.*, **92**, 13,407–13,420, 1988.

Minoura, K., F. Imamura, D. Sugawara, Y. Kono, and T. Iwashita, The 869 Jogan tsunami deposit and recurrence interval of large-scale tsunami on the Pacific coast of northeast Japan, *J. Natural Disaster Sci.*, **23**(2), 83–88, 2001.

Pelayo, A. M. and D. A. Wiens, Tsunami earthquakes: Slow thrust-faulting events in the accretionary wedge, *J. Geophys. Res.*, **97**, 15,321–15,337, 1992.

Polet, J. and H. Kanamori, Shallow subduction zone earthquakes and their tsunamigenic potential, *Geophys. J. Int.*, **142**, 684–702, 2000.

Stauder, W., Mechanism of the Rat Island earthquake sequence of February 4, 1965 with relation to island arcs and sea-floor spreading, *J. Geophys. Res.*, **73**, 3847–3858, 1968.

Takahaski, N., S. Kodaira, T. Tsuru, J.-O. Park, Y. Kaneda, K. Suyehiro, H. Kinoshita, S. Abe, M. Nishino, and R. Hino, Seismic structure and seismogenesis off Sanriku region, northeastern Japan, *Geophys. J. Int.*, **159**, 129–145, 2004.

Tanioka, Y. and K. Satake, Fault parameters of the 1896 Sanriku tsunami earthquake estimated from tsunami numerical modeling, *Geophys. Res. Lett.*, **23**, 1549–1552, 1996.

Tanioka, Y. and T. Seno, The sediment effect on tsunami generation of the 1896 Sanriku tsunami earthquake, *Geophys. Res. Lett.*, **28**, 3389–3392, 2001.

Taylor, M. A. J., G. Zheng, J. R. Rice, W. D. Stuart, and R. Dmowska, Cyclic stressing and seismicity at strong coupled subduction zones, *J. Geophys. Res.*, **101**, 8363–8381, 1996.

T. Lay (e-mail: tlay@ucsc.edu), C. J. Ammon, H. Kanamori, M. J. Kim, and L. Xue